Journal of Alloys and Compounds 512 (2012) 121–123

Contents lists available at SciVerse ScienceDirect

Journal of Alloys and Compounds

journal homepage: www.elsevier.com/locate/jallcom

Impact of Ce^{4+} ion on microstructure and luminescence character of Ho^{3+}/Yb^{3+} co-doped ZrO_2 nanocrystal

Chengguo Ming[a,b,*], Feng Song[b,c,**], Yin Yu[b,c], Qingru Wang[b,c]

[a] Physics Department, School of Sciences, Tianjin University of Science & Technology, Tianjin 300222, China
[b] The Key Laboratory of Weak Light Nonlinear Photonics, Ministry of Education, Nankai University, Tianjin 300457, China
[c] School of Physics, Nankai Univeristy, Tianjin 300071, China

ARTICLE INFO

Article history:
Received 4 August 2010
Received in revised form
11 September 2011
Accepted 14 September 2011
Available online 19 September 2011

Keywords:
Ho^{3+}/Yb^{3+} co-doped
Up-conversion emission
Solid-state synthesis method

ABSTRACT

By solid-state synthesis method, Ho^{3+}/Yb^{3+} co-doped CeO_2–ZrO_2 nano-powders have been prepared. The concentration of Ce^{4+} ions has greater effect to the oxygen lattice structure. When the concentration of Ce^{4+} ions is 30 mol%, the oxygen lattice is a tetrahedral space group and the luminescence intensity of the sample is strongest. The results show that the lattice structure can be changed by inducting the Ce^{4+} ions into Ho^{3+}/Yb^{3+} co-doped ZrO_2. And the emission character can be improved.

1. Introduction

In recent decades, the visible light luminescence materials have widely been applied to color display, white light simulation, up-conversion (UC) laser [1–3], and so on. In view of the abundant energy level of rare earth ions in the visible range, the rare earth ions doped materials have attracted people's interest [4–7]. For improving the emission intensity and efficiency of the materials, many hosts have been investigated, such as glasses and crystals. Glass hosts usually have lower emission efficiency (silicate and phosphate), poor thermal stability and chemical durability (fluoride and telluride). Crystal materials own good physical, chemical character and high emission efficiency. Especially, the preparation technology of the nano-powders is easier and its product cost is lower, which are more suitable for industrial production. For finding better luminescence character, people make a lot of research for rare earth ions doped ZrO_2 nano-powder [8–10]. The pure ZrO_2 lattice is usually tetragonal structure. When an amount of rare earth ions is introduced, only cubic phase can be observed [11]. In different crystal field, the luminescence character of rare earth ions is different. In this letter, we prepared Ho^{3+}/Yb^{3+} co-doped CeO_2–ZrO_2 nano-powders. The impact of Ce^{4+} ions on microstructure and luminescence character of Ho^{3+}/Yb^{3+} co-doped ZrO_2 nano-crystal have been studied.

2. Experimental

The powder samples with the composition of $x CeO_2$–$(0.90-x)ZrO_2$–$0.01Ho_2O_3$–$0.04Yb_2O_3$ (mol%) were prepared by solid-state synthesis method. The samples with $x = 0$, 0.10, 0.30, 0.50, 0.70, 0.90 are numbered as ZC1, ZC2, ZC3, ZC4, ZC5, ZC6. The raw materials, consisting of reagent grade $Zr(NO_3)_4{\cdot}5H_2O$, CeO_2, Ho_2O_3 and Yb_2O_3, were mixed thoroughly. Initially, the furnace was heated to 600 K at the rate of 1 K min^{-1} and held at the temperature for 3 h to release the volatile components. Finally, the furnace temperature was raised to 1700 K at the rate of 2 K min^{-1} and control at the temperature for 2 h. Finally, the samples were grounded into fine powder for optical measurements.

XRD were obtained by a Bruker AXSB8 Discover model using Cu K_α radiation ($\lambda = 0.154$ nm). The scan rate of 0.05° min^{-1} was used to record a pattern in the 2θ range of 20–80°. Raman spectra were obtained with an Invia Raman Mircoscope. The photoluminescence spectra under excitation light from a 975 nm laser diode (LD) and a xenon (Xe) lamp were measured with a model F111AI fluorescence spectrophotometer. All the measurements were taken at room temperature.

3. Results and discussion

3.1. XRD analysis

Fig. 1 is the XRD patterns of the powder samples ZC1–ZC6. The diffraction peaks of the sample ZC1 come from the reflections of $Yb_{0.1}Zr_{0.9}O_{1.95}$. Its oxygen lattice is a cubic $Pm\bar{3}m$ (255) space group. The Yb^{3+} ion has replaced the Zr^{4+} ion of ZrO_2 crystal lattice. For samples ZC2 and ZC3, the diffraction peaks originate from the $Yb_{0.2}Zr_{0.8}O_{1.9}$ and $Zr_3Yb_4O_{12}$. Their oxygen lattices are

* Corresponding author at: Physics Department, School of Sciences, Tianjin University of Science & Technology, Tianjin 300222, China.
** Corresponding author at: Photonics Center, The Key Laboratory of Weak Light Nonlinear Photonics, Ministry of Education, Nankai University, Tianjin 300457, China. Fax: +86 22 2350 1743.
E-mail addresses: mingchengguo1978@163.com (C. Ming), fsong@nankai.edu.cn (F. Song).

0925-8388/$ – see front matter © 2011 Elsevier B.V. All rights reserved.
doi:10.1016/j.jallcom.2011.09.035

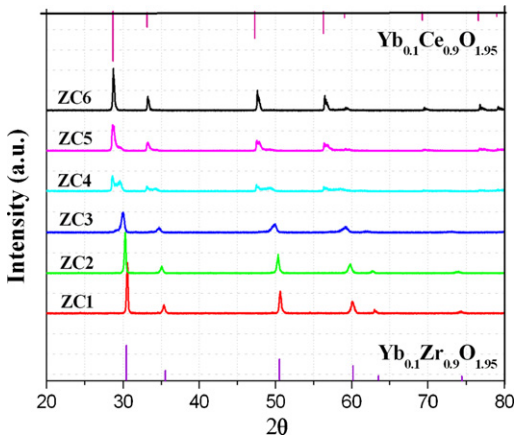

Fig. 1. XRD patterns of the powder samples ZC1–ZC6. The bars in the diagram above and below are the standard patterns of $Yb_{0.1}Ce_{0.9}O_{1.95}$ and $Yb_{0.1}Zr_{0.9}O_{1.95}$.

the cubic $Pm\bar{3}m$ (255) and tetrahedral $R\bar{3}$ (148) space groups. For samples ZC5 and ZC6, the diffraction peaks due to the reflections of $Yb_{0.1}Ce_{0.9}O_{1.95}$, which is the cubic $Fm\bar{3}m$ (225) space groups. As for the sample ZC4, besides the diffraction peaks of $Yb_{0.1}Ce_{0.9}O_{1.95}$, the else peaks come from the reflections of $CeZrO_2$. With the increasing of Ce^{4+} ions doped concentration, the diffraction peak intensities of $Yb_xZr_yO_z$ decrease gradually and the position of diffraction peaks moves to the small angle. The diffraction peak intensities of $Yb_{0.1}Ce_{0.9}O_{1.95}$ increase gradually. The results show that the crystal structure can vary from the cube to the tetrahedron by the larger size of the Ce^{4+} (0.1034 nm) ion substituting the Zr^{4+} (0.0720 nm) ion in the crystal lattice. But when the concentration of Ce^{4+} ions is larger, the lattice turns into the cubic structure again.

3.2. Raman spectra

Fig. 2 is the Raman and luminescence emission spectra of the Ho^{3+}/Yb^{3+} co-doped samples under 514 nm Ar laser excitation. The emission peaks located at Stokes shifts lower than 700 cm^{-1} from the excitation line should be assigned to Raman active lattice phonon. For sample ZC1 (the single ZrO_2 host), the Raman peaks appear at 635, 472, 501, 256, 145 cm^{-1} (see the inset of Fig. 2). The sharp Raman peak at 462 cm^{-1} comes from the F_{2g} vibration of the

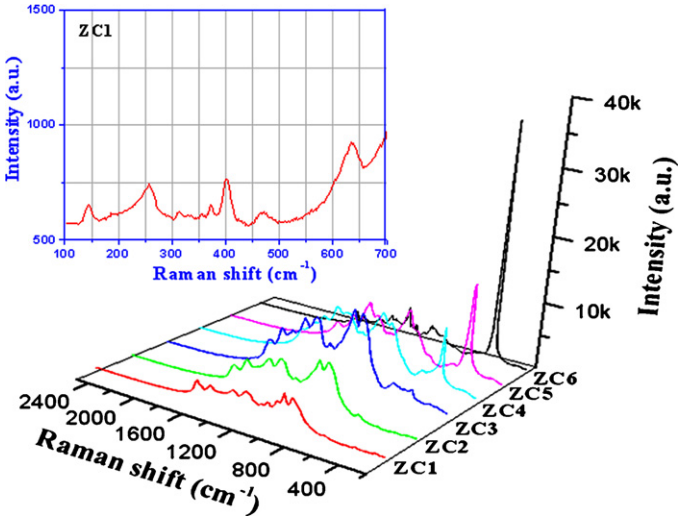

Fig. 2. Raman and luminescence spectra of the Ho^{3+}/Yb^{3+} co-doped samples ZC1–ZC6 (λ_{ex} = 514 nm). The inset is the Raman spectra of the sample ZC1 in 100–700 cm^{-1} wavenumber range.

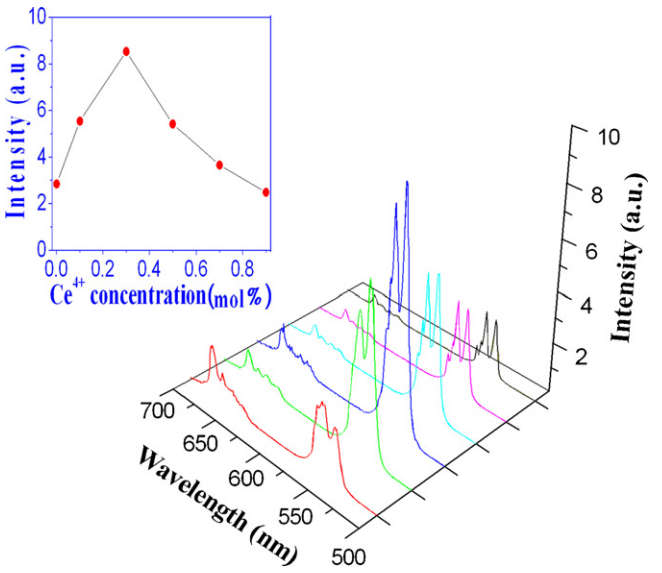

Fig. 3. UC emission of the samples ZC1–ZC6 at 975 nm LD excitation, the inset is the intensity of the green emission depends on the concentration of Ce^{4+} ions. (For interpretation of the references to color in this figure legend, the reader is referred to the web version of the article.)

fluorite type lattice of CeO_2 [12]. The strong and wide emission band higher than 700 cm^{-1} cannot be ascribed to vibrative modes. It should be due to electronic emission transitions of Ho^{3+} ions: $^5F_4, {}^5S_2 \rightarrow {}^5I_8$. At 514 nm light excitation, the emission intensity of Ho^{3+} ions in the samples ZC1–ZC6 (the concentration of Ce^{4+} ions increases in turn) firstly increases, then decrease. As for the Raman active lattice phonon spectra, under lower Ce^{4+} doped concentration, the Raman peaks are very weak, which are overlapped by the strong emission band of Ho^{3+} ions. But with the increasing of Ce^{4+} doped concentration, the 462 cm^{-1} Raman peak becomes stronger and stronger. Finally, the intensity of the Raman peak is stronger compared to that of emission peak of Ho^{3+} ions.

3.3. Emission character

Fig. 3 is the UC emission of the Ho^{3+}/Yb^{3+} co-doped samples at 975 nm LD excitation. The UC green emission (at 525–570 nm wavelength band) and the UC red emission (at 640–680 nm wavelength band) were observed, which come from the transition of Ho^{3+} ions: $^5F_4, {}^5S_2 \rightarrow {}^5I_8$ and $^5F_5 \rightarrow {}^5I_8$, respectively. For the sample ZC1 (with the single ZrO_2 host), the intensities of the green emission and the red emission are lower. With the increasing of Ce^{4+} ions concentration, the intensity of the UC green emission firstly increases, then gradually decreases. But the intensity of the UC red emission did not obviously change. The green emission intensity of the sample ZC3 (with 30 mol% CeO_2) is strongest, see the inset of Fig. 3. The reason can be interpreted as following: for samples ZC1, ZC2, ZC4, ZC5 and ZC6, their oxygen lattices are the cubic structure. Ho_2O_3 lattice is also a cubic space group. The good Ho^{3+} site symmetry decreases the electric dipole transition probability. Therefore, the luminescence intensity is lower. The metal ions in the sample ZC3 is a hexagonal structure and *f–f* electric dipole transitions of the Ho^{3+} ions can become allowed. The results show that the UC green emission can be obviously improved by Ce^{4+} ions doping in the Ho^{3+}/Yb^{3+} co-doped ZrO_2 powder. The best Ce^{4+} ions doped concentration is 30 mol%.

Fig. 4 is the luminescence spectra of the Ho^{3+}/Yb^{3+} co-doped samples at Xe-lamp (λ_{ex} = 449 nm) excitation. The green emission is very strong and the red emission can hardly be observed. The result shows that the population of the $^5F_5$ energy level did not

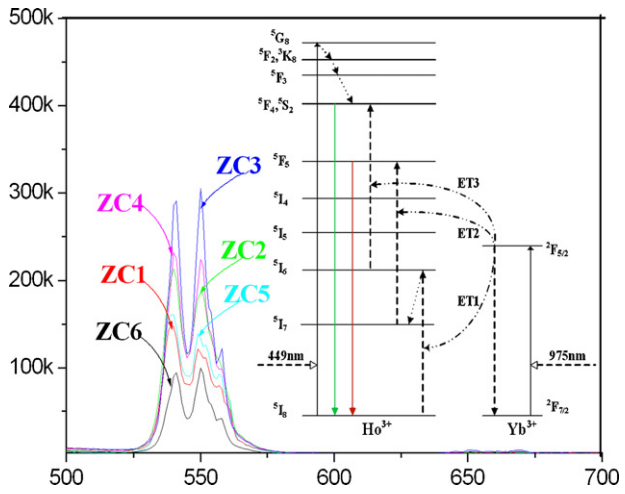

Fig. 4. Emission spectra of Ho^{3+}/Yb^{3+} co-doped samples at 449 nm light excitation. The inset is the energy diagram of Ho^{3+} and Yb^{3+} ions, as well as the proposed energy transition processes.

come from the non-radiative transition of the $^5F_4$ energy level. With the increasing of Ce^{4+} ions concentration, the variation law of the green emission intensity at 449 nm light excitation is in agreement with that at 975 nm LD pumping.

The energy level diagrams of Yb^{3+} and Ho^{3+} is shown in the inset of Fig. 4 under the excitation of 975 nm LD and 449 nm Xe-lamp. At 975 nm LD pumping, the population processes of the UC green emission can be described as the following: by energy transition (ET) 1: $^2F_{5/2}(Yb^{3+}) + {}^5I_8(Ho^{3+}) \rightarrow {}^2F_{7/2}(Yb^{3+}) + {}^5I_6(Ho^{3+})$ and ET2: $^2F_{5/2}(Yb^{3+}) + {}^5I_6(Ho^{3+}) \rightarrow {}^2F_{7/2}(Yb^{3+}) + {}^5F_4, {}^5S_2(Ho^{3+})$, the Ho^{3+} ions in the ground state transferred to $^5F_4$, $^5S_2$ states, from where the green emission arises. The population of the UC red emission is: by ET1, the Ho^{3+} ions are excited to $^5I_6$ state. The ions relax to $^5I_7$ state by mult-phonon relaxation. Then by ET3: $^2F_{5/2}(Yb^{3+}) + {}^5I_7(Ho^{3+}) \rightarrow {}^2F_{7/2}(Yb^{3+}) + {}^5F_5(Ho^{3+})$, the ions are pumped to $^5F_5$ state, from where the red emission arises. But because of the low phonon energy of the samples (the largest phonon energy is 635 cm^{-1}), the mult-phonon relaxation probability from $^5I_6$ to $^5I_7$ energy level (the energy gap 3500 cm^{-1}, about 5-phonon process) is very lower. This is the reason that the UC red emission is very weak. At 449 nm light excitation, the population processes of the green emission is very manifest. The Ho^{3+} ions in the ground state transfer to $^5G_8$ state by ground state absorption: $^5I_8(Ho^{3+}) + h\nu \rightarrow {}^5G_8(Ho^{3+})$. Subsequently, by mult-phonon relaxation, the ions relax to $^5F_4$, $^5S_2$ states.

4. Conclusions

By solid-state synthesis method, we prepared a series of Ho^{3+}/Yb^{3+} co-doped CeO_2–ZrO_2 powders. The Ce^{4+} ions concentration has greater impact on the oxygen lattice structure. When the concentration of Ce^{4+} ions is 30 mol%, the lattice is the tetrahedral space group. This work will be helpful for developing luminous material.

Acknowledgments

This work was supported by the Natural Nature Science Foundation of China (No. 90923035), and the Program for Innovative Research Team in University. We'd like to thank Mr. Liqun An for his kind help in the English grammar.

References

[1] E. Downing, L. Hesseink, J. Ralston, R. Macfarlane, Science 273 (1996) 1185–1189.
[2] S. Tokito, T. Lijima, T. Tsuzuki, F. Sato, Appl. Phys. Lett. 83 (2003) 2459–2461.
[3] L. Han, F. Song, S.Q. Chen, C.G. Zou, X.C. Yu, J.G. Tian, J. Xu, X. Xu, G. Zhao, Appl. Phys. Lett. 93 (2008) 011110-1–011110-3.
[4] J.C. Boyer, L.A. Cuccia, J.A. Capobianco, Nano Lett. 7 (2007) 847–852.
[5] X.C. Yu, F. Song, W.T. Wang, L.J. Luo, C.G. Ming, Z.Z. Cheng, L. Han, T.Q. Sun, H. Yu, J.G. Tian, Opt. Commun. 282 (2009) 2045–2048.
[6] Z.C. Duan, J.J. Zhang, W.D. Xiang, H.T. Sun, L.L. Hu, Mater. Lett. 61 (2007) 2200–2202.
[7] Z. Pan, A. Ueda, R. Mu, S.H. Morgan, J. Lumin. 126 (2007) 251–256.
[8] A. Patra, C.S. Friend, R. Kapoor, P.N. Prasad, J. Phys. Chem. B 106 (2002) 1909–1912.
[9] P. Salas, C. Angeles-Chávez, J.A. Montoya, E. De la Rosa, L.A. Diaz-Torres, H. Desirena, A. Martínez, M.A. Romero-Romo, J. Morales, Opt. Mater. 27 (2005) 1295–1300.
[10] R.K. Jia, W.S. Yang, Y.B. Bai, T.J. Li, Opt. Mater. 28 (2006) 246–251.
[11] G.Y. Chen, G. Somesfalean, Y. Liu, Z.G. Zhang, Q. Sun, F.P. Wang, Phys. Rev. B 75 (2006) 195204-1–195204-6.
[12] A. Martinez-Arias, M. Fernandez-Garcia, L.N. Salamanca, R.X. Valenzuela, J.C. Conesa, J. Soria, J. Phys. Chem. B 104 (2000) 4038–4046.